ChemComm

Accepted Manuscript

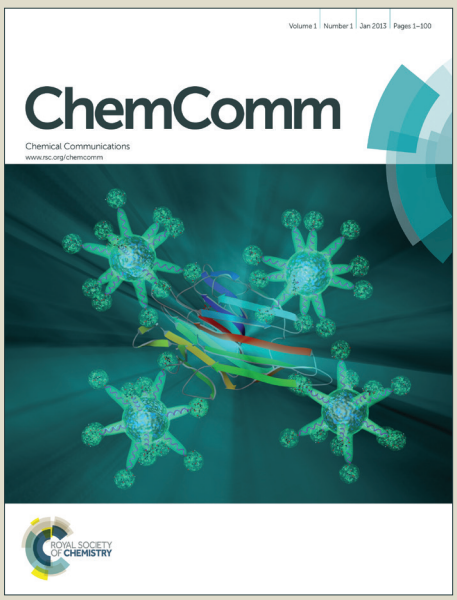

This is an *Accepted Manuscript*, which has been through the Royal Society of Chemistry peer review process and has been accepted for publication.

Accepted Manuscripts are published online shortly after acceptance, before technical editing, formatting and proof reading. Using this free service, authors can make their results available to the community, in citable form, before we publish the edited article. We will replace this *Accepted Manuscript* with the edited and formatted *Advance Article* as soon as it is available.

You can find more information about *Accepted Manuscripts* in the Information for Authors.

Please note that technical editing may introduce minor changes to the text and/or graphics, which may alter content. The journal's standard Terms & Conditions and the Ethical guidelines still apply. In no event shall the Royal Society of Chemistry be held responsible for any errors or omissions in this *Accepted Manuscript* or any consequences arising from the use of any information it contains.

ROYAL SOCIETY OF CHEMISTRY

www.rsc.org/chemcomm

Journal Name

RSCPublishing

COMMUNICATION

Facile synthesis of 3D Pd-P nanoparticle networks with enhanced electrocatalytic performance towards formic acid electrooxidation

Cite this: DOI: 10.1039/x0xx00000x

Received 00th January 2012,
Accepted 00th January 2012

DOI: 10.1039/x0xx00000x

www.rsc.org/

Jingfang Zhang, You Xu and Bin Zhang*

3D Pd-P nanoparticle networks (NNs) have been successfully synthesized using a facile one-step soft-template-assisted method. The as-prepared Pd-P NNs exhibit markedly improved activity and stability towards formic acid electrooxidation over Pd NNs, commercial Pd/C and Pd-P nanoparticle aggregates (NAs).

Direct formic acid fuel cells (DFAFCs) have attracted considerable research interest as a new generation of environment-friendly power source due to their high energy density, limited fuel crossover, high electromotive force and low operating temperature.[1] The rapid development of DFAFCs in the past decade has stimulated the intensive research in the design and synthesis of excellent electrocatalysts for formic acid electro-oxidation reaction (FAER). Pd-based composites are considered as effective electrocatalysts towards FAER for their lower cost and higher activity compared to Pt-based catalysts.[2] However, pure Pd catalysts suffer from a fatal drawback of slow deactivation during FAER due to either the oxidation of Pd surface or the catalyst poisoning.[3] Thus, it is desirable to develop new Pd-based electrocatalysts with higher activity and extended durability. Recent studies have indicated the doped non-metal element P with abundant valence electrons can improve the electrocatalytic activities and CO tolerances effectively.[4,5] However, the development of synthetic methodology to control the morphology and structure of such P doped Pd-based nanostructures, which are linked to the properties with a greater versatility, imposes important challenges. In particular, metal-based nanoparticle networks (NNs) are considered to be promising electrocatalysts candidates because the combination of net-like feature and nanoparticle blocks can achieve both the construction of self-supported electrocatalysts and the retain of nanoparticle's high activity.[6] Moreover, the NNs can not only increase the active area accessible to the reactant molecules, but also provide effective electron mobility in the solid ligaments as well as efficient mass transfer in the catalytic reactions.[6] Furthermore, abundant defect sites and low-coordination atoms on the nanoparticle surfaces are favorable active sites for organic small molecule electro-oxidation.[6]

Herein, we reported a facile and efficient one-step soft-template-assisted strategy to prepare 3D Pd-P alloy NNs with sub-10 nm nanoparticles as building blocks. The as-prepared Pd-P NNs are found to exhibit excellent electrocatalytic activity and stability towards FAER.

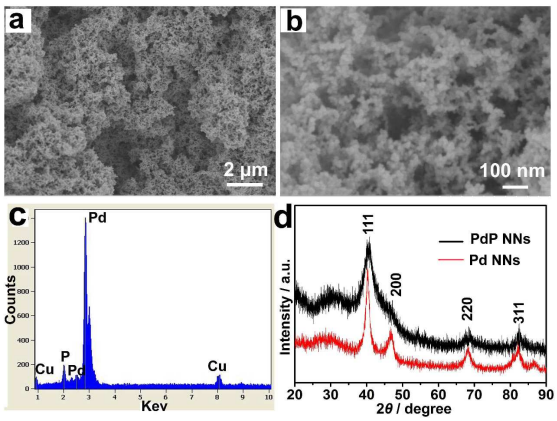

Fig. 1 (a, b) Low- and high-magnification SEM images of Pd-P NNs. (c) EDX spectrum of Pd-P NNs. The detected Cu singles arise from the Cu foil on which the samples were deposited. (d) XRD patterns of Pd-P NNs and Pd NNs.

The 3D Pd-P alloy NNs were prepared through the hydrothermal reaction of Na_2PdCl_4 and NaH_2PO_2 in the presence of HCHO as reducing agent and Brij 58 as soft template (see experimental details in ESI†). The as-obtained samples were firstly characterized by using scanning electron microscopy (SEM). As shown in Fig. 1a, the samples with 3D NNs could be prepared on a large scale. The high-magnification SEM image (Fig. 1b) further confirms the network-like feature composed of many nanoparticles. The energy dispersive X-ray (EDX)

ChemComm Accepted Manuscript

spectroscopy (Fig. 1c) also indicates that the as-prepared networks are composed of Pd and P with the atomic ratio of 7.5:1 (Pd to P). In the absence of NaH_2PO_2 with other conditions remain unchanged, the as-produced samples are pure Pd NNs (ESI, Fig. S1†). X-ray diffraction (XRD) patterns in Fig. 1d show that both Pd-P NNs and Pd NNs exhibit diffraction peaks of a face centered cubic crystal structure (JCPDS 05-0681).[7] In comparison to pure Pd NNs, it is found that the corresponding diffraction peaks of Pd-P NNs shift to the higher 2θ degrees, suggesting the lattice contraction due to the partial substitution of Pd by P.[4d] In addition, the diffraction peaks of the Pd-P NNs are much broader than those of the Pd NNs, showing that the average particle size of Pd-P NNs is much smaller than that of Pd NNs. According to the Scherrer formular[4d], the average sizes of Pd-P and Pd NNs are calculated to be 3.3 nm and 7.7 nm, respectively. In other words, the addition of P reduces the particle size of Pd-P NNs.

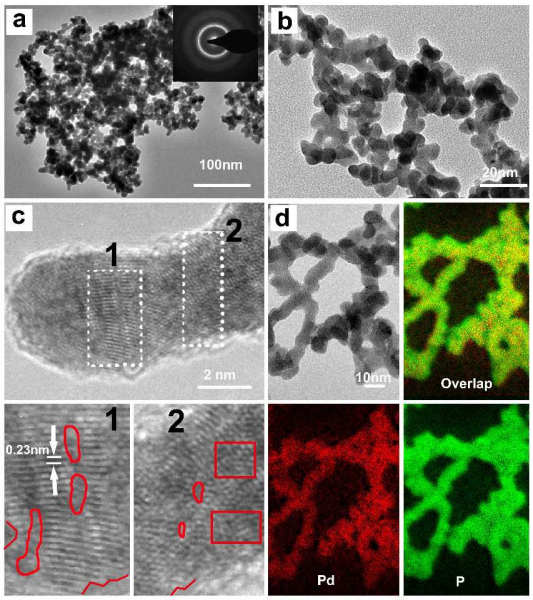

Fig. 2 (a) and (b) TEM images of Pd-P NNs. Insert in (a): SAED pattern. (c) HRTEM image of Pd-P NNs. The areas marked in Fig. 2c1-2 are many defects with vacancy (by red circles), dislocation (by red squares), as well as several atomic steps and corners (by red lines). (d) Representative TEM image of Pd-P NNs and corresponding EDX mapping images of Pd (red) and P (green) elements.

The structural features were further investigated by the transmission electron microscopy (TEM). As shown in Fig. 2a,b, it is clearly seen that the NNs are composed of interconnected nano-particles with a diameter of 2-8 nm. TEM images of pure Pd NNs are shown in Fig. S2 (ESI†). The selected area electron diffraction (SAED) pattern (the insert in Fig. 2a) indicates the polycrystalline character of Pd-P NNs. To better understand the crystalline characteristics of the Pd-P NNs, high resolution TEM (HRTEM) measurements of a typical single particle were conducted (Fig. 2c). The clear fringes in the HRTEM image show the lattice spacing of 0.23 nm corresponding to that of fcc Pd (111) planes.[7,8] In the marked **1** and **2** areas in Fig. 2c, there are many defects with vacancy, dislocations, as well as several atomic steps and corners. These defects can act as highly catalytic active sites for significantly enhanced activity.[9] The EDX mapping in Fig. 2d clearly reveals that Pd and P are uniformly distributed throughout the entire nanostructure. All measurements above suggest the successful synthesis of Pd-P NNs.

The surface composition of Pd-P NNs was further analyzed by X-ray photoelectron spectroscopy (XPS) (ESI, Fig. S3† and Fig. 3). In the P 2p spectrum of Pd-P NNs (Fig. 3a), the P 2p peaks at 129.9 and 133.1 eV are assigned to elemental state phosphorus and oxidized phosphorus,[5] respectively. In the Pd 3d spectrum of Pd-P NNs (Fig. 3b), the Pd 3d signal of Pd-P NNs is fitted to two pairs of doublets with a spin-orbit separation of 5.3 eV: Pd $3d_{3/2}$ (341.2 eV), Pd $3d_{5/2}$ (335.9 eV) and Pd $3d_{3/2}$ (342.2 eV), Pd $3d_{5/2}$ (336.9 eV), which can be assigned to Pd^0 and Pd^{II}, respectively. The energy of Pd^0 and Pd^{II} in Pd-P NNs positively shift ca. 0.4 eV compared to that of pure Pd.[5] This may be due to the fact that the interacting role of Pd with P makes positively charged Pd donate electrons and thus it leads to a decrease of the 3d electron density of Pd atom in Pd-P NNs.[5]

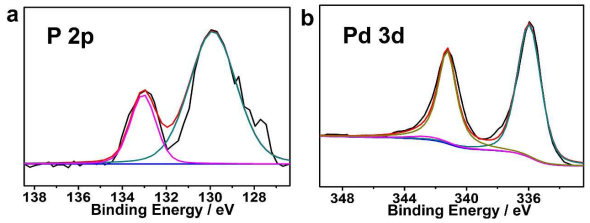

Fig. 3 XPS spectra of P 2p (a) and Pd 3d (b) of Pd-P NNs.

To probe the intrinsic factors influencing the formation of the Pd-P NNs, a series of control experiments were carried out. Time-dependent experiments show that many clusters consisted of small nanoparticles were formed in 1 h, and these clusters began to contact together to form chain-like aggregates (ESI, Fig. S4a†). When the reaction time was prolonged, the chain-like structures in 2 h and the NNs in 4 h were obtained (ESI, Fig. S4b,c†). By further increasing the reaction time, the NNs feature became more and more obvious (ESI, Fig. S4d,e†). The P content also enlarged with more reaction time (ESI, Fig. S4f†). Interestingly, the P content could be increased by increasing the amount of added P source (ESI, Fig. S5†). Moreover, the reaction temperature has a noticeable influence on the network-like morphology and the size of nanoparticles of the products (ESI, Fig. S6†). Furthermore, it is found that the presence of Brij 58 is critical for the formation of Pd-P NNs (ESI, Figure S7†).[10] Note that the detailed growth mechanism of Pd-P NNs need to be further investigated.

FAER was used to characterize the electrocatalytic activity of the as-prepared Pd-P NNs while Pd NNs and Pd/C are used for comparison. Fig. 4a shows the cyclic voltammograms (CVs) of the three catalysts recorded in 0.5 M H_2SO_4 at 50 mV s^{-1}. The electrochemically active surface areas (ECSAs) are calculated to be 18.92, 12.16 and 16.01 $m^2\ g_{Pd}^{-1}$ for Pd-P NNs, Pd NNs and Pd/C catalysts, respectively. Fig. 4b displays the CVs of three catalysts in 0.5 M HCOOH + 0.5 M H_2SO_4 solutions. The forward peak current density for FAER on Pd-P NNs is 3.22 mA cm^{-2},

ChemComm Accepted Manuscript

This journal is © The Royal Society of Chemistry 2012

which is about 1.39 and 3.62 times than that of Pd NNs (2.32 mA cm^{-2}) and Pd/C (0.89 mA cm^{-2}). Meanwhile, the corresponding mass activity of three catalysts were also tested (ESI, Fig. S8a and Table S1†). This indicates that Pd-P NNs exhibit markedly enhanced electrocatalytic activity toward FAER. The electrochemical stability of Pd-P NNs was studied by chronoamp-erometry at 0.1 V (Fig. 4c; ESI, Fig. S8b†). It is found that the Pd-P NNs exhibit a slower current decay and much higher current densities than Pd NNs and Pd/C catalysts, indicating a higher tolerance to the

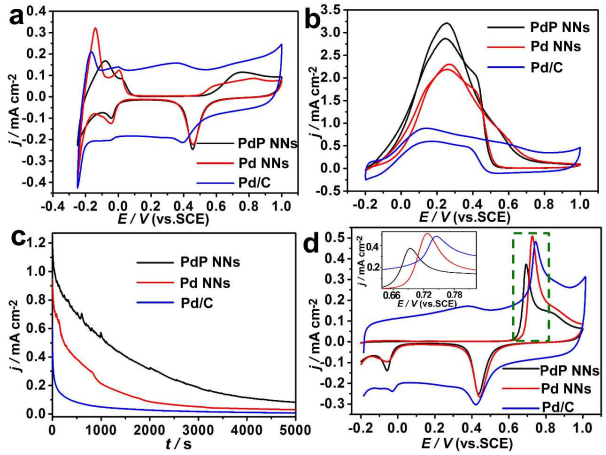

Fig. 4 (a) CVs of Pd-P NNs, Pd NNs and Pd/C in 0.5 M H_2SO_4 at 50 mV s^{-1}. (b, c) CVs (b) and Chronoamperometry curves (c) of Pd-P NNs, Pd NNs and Pd/C in 0.5 M HCOOH + 0.5 M H_2SO_4 at 50 mV s^{-1}. (d) CO stripping measurements of Pd-P NNs, Pd NNs and Pd/C in 0.5 M H_2SO_4 at 50 mV s^{-1} in the first forward scan. Inserts: magnified area enclosed with green squares.

intermediate poisoning species generated from FAER, thus better catalytic ability of Pd-P NNs toward FAER. In addition, the electrochemical durability of the Pd-P NNs was evaluated. As shown in Fig. S9 (ESI†), the CV measurements show a loss of 12.5% for Pd-P NNs and 45.0% for Pd/C in ECSAs after 1000 potential cycles, revealing that the durability of Pd-P NNs is also better than the Pd/C catalyst. While serious aggregation was observed for Pd/C, the morphology of the Pd-P NNs was still largely maintained after durability tests. Meanwhile, the sintering-induced mass activity loss was studied (ESI, Fig. S10†). The activities Pd-P samples with different atomic ratios are compared (ESI, Fig. S11†). The optimized atomic ratio is 7.5:1 (Pd to P). CO stripping measurements were applied to exhibit the antipoisoning ability of catalysts.[11] In Fig. 4d and Fig. S12 (ESI†), the peak potential (0.69 V) of CO oxidation on the Pd-P NNs is obviously more negative than that of the Pd NNs (0.73 V) and commercial Pd/C (0.74 V). XPS results suggest that the incorporation of P into Pd lowers the 3d electron density of Pd and makes formic acid be easily oxidized through the direct pathway, which partly accounts for the high catalytic activity.[5] Furthermore, the advantages of 3D Pd-P NNs over Pd-P nanoparticles aggregates (named Pd-P NAs here; ESI, Fig. S7d and S13†) can be confirmed on the basis of a series of electrochemical measurements (ESI, Fig. S14†). The catalytic enhancement of Pd-P NNs may be attributed to the exposure of their intrinsic active sites and larger ECSA provided by 3D networks,[6,9] as well as the synergetic effects between Pd and P.[4]

In summary, we have demonstrated a facile one-step soft-template-assisted synthesis of 3D Pd-P NNs with sub-10 nm nanoparticles as building blocks. It is found that the as-prepared Pd-P NNs exhibit markedly improved activity and stability towards FAER over Pd NNs, commercial Pd/C and Pd-P NAs, which may be associated with the unique 3D networks and the electronic effects between Pd and P. Importantly, this work will provide a new synthetic strategy to construct other P-doped multimetallic networks, which may be promising candidates for advanced catalytic applications.

The work was financially supported by NSFC (No.21373149).

Notes and references

Department of Chemistry, School of Science, Tianjin University, and Collaborative Innovation Center of Chemical Science and Engineering (Tianjin), Tianjin 300072, China. E-mail: bzhang@tju.edu.cn

† Electronic supplementary information (ESI) available: Experimental procedures and additional characterization results. See DOI: 10.1039/c000000x/

1 a) C. V. Rao, C. R. Cabrera and Y. Ishikawa, *J. Phys. Chem. C*, 2011, **115**, 21963; b) H. Lee, S. E. Habas, G. A. Somorjai and P. Yang, *J. Am. Chem. Soc.*, 2008, **130**, 5406; c) L. Dai and S. Zou, *J. Power Sources*, 2011, **196**, 9369.

2 a) V. Mazumder and S. Sun, *J. Am. Chem. Soc.*, 2009, **131**, 4588; b) E. Antolini, *Energy Environ. Sci.*, 2009, **2**, 915.

3 a) X. Liu, D. Wang and Y. Li, *Nano Today*, 2012, **7**, 448; b) L. Zhang, J. Zhang, Q. Kuang, S. Xie, Z. Jiang, Z. Xie and L. Zheng, *J. Am. Chem. Soc.*, 2011, **133**, 17114; c) A. K. Singh and Q. Xu, *ChemCatChem*, 2013, **5**, 652.

4 a) S. H. Lee, D. J. Kim and Y. S. Yoon, *Jpn. J. Appl. Phys.*, 2013, **52**, 035001; b) S. Suzuki, Y. Ohbu, T. Mizukami, Y. Takamori, M. Morishima, H. Daimon and M. Hiratani, *J. Electrochem. Soc.*, 2009, **156**, B27; c) A. F. Shao, Z. B. Wang, Y. Y. Chu, Z. Z. Jiang, G. P. Yin and Y. Liu, *Fuel Cells*, 2010, **3**, 472; d) L. Cheng, Z. Zhang, W. Niu, G. Xu and L. Zhu, *J. Power Sources*, 2008, **182**, 91.

5 H. Sun, J. Xu, G. Fu, X. Mao, L. Zhang, Y. Chen, Y. Zhou, T. Lu and Y. Tang, *Electrochim. Acta*, 2012, **59**, 279.

6 a) Y. Xu and B. Zhang, *Chem. Soc. Rev.*, 2014, **43**, 2439; b) R. Wang, C. Xu, X. Bi and Y. Ding, *Energy Environ. Sci.,* 2012, **5**, 5281; c) S. Ge, F. Liu, W. Liu, M. Yan, X. Song and J. Yu, *Chem. Commun.*, 2014, **50**, 475; d) Y. B. Cho, J. E. Kim, J. H. Shim, C. Lee and Y. Lee, *Phys. Chem. Chem. Phys.*, 2013, **15**, 11461; e) Z. Y. Shih, C. W. Wang, G. Xu and H. T. Chang, *J. Mater. Chem. A*, 2013, **1**, 4773; f) L. Liu, R. Scholz, E. Pippel and U. Gösele, *J. Mater. Chem.*, 2010, **20**, 5621; g) D. Wen, A. K. Herrmann, L. Borchardt, F. Simon, W. Liu, S. Kaskel and A. Eychmüller, *J. Am. Chem. Soc.*, 2014, **136**, 2727; h) G. Duan, W. Cai, Y. Luo, F. Lv, J. Yang and Y. Li, *Langmuir*, 2009, **25**, 2558.

7 X. Huang, Y. Li, Y. Chen, E. Zhou, Y. Xu, H. Zhou, X. Duan and Y. Huang, *Angew. Chem. Int. Ed.*, 2013, **52**, 2520.

8 a) J. Chang, L. Feng, C. Liu, W. Xing and X. Hu, *Angew. Chem. Int. Ed.*, 2014, **53**, 122; b) W. Liu, A. K. Herrmann, D. Geiger, L. Borchardt, F. Simon, S. Kaskel, N. Gaponik and A. Eychmüller,

ChemComm Accepted Manuscript

Angew. Chem. Int. Ed., 2012, **51**, 1; c) F. R. Fan, A. Attia, U. K. Sur, J. B. Chen, Z. X. Xie, J. F. Li, B. Ren and Z. Q. Tian, *Cryst. Growth Des.*, 2009, **9**, 2335.

9 a) L. Zhang, D. Lu, Y. Chen, Y. Tang and T. Lu, *J. Mater. Chem. A*, 2014, **2**, 1252; b) J. Zhang, H. Yang, J. Fang and S. Zou, *Nano Lett.*, 2010, **10**, 638; c) H. Zhang, M. Jin and Y. Xia, *Angew. Chem. Int. Ed.*, 2012, **51**, 7656; d) J. Watt, N. Young, S. Haigh, A. Kirkland and R. D. Tilley, *Adv. Mater.*, 2009, **21**, 2288; e) Y. Wu, D. Wang, X. Chen, G. Zhou, R. Yu and Y. Li, *J. Am. Chem. Soc.*, 2013, **135**, 12220.

10 H. Wang, S. Ishihara, K. Ariga and Y. Yamauchi, *J. Am. Chem. Soc.*, 2012, **134**, 10819.

11 L. X. Ding, C. L. Liang, H. Xu, A. L. Wang, Y. X. Tong and G. R. Li, *Adv. Mater. Interfaces*, 2014, DOI: 10.1002/admi.201400005.

ChemComm Accepted Manuscript

 This journal is © The Royal Society of Chemistry 2012

Graphic Abstract

Facile synthesis of 3D Pd-P nanoparticle networks with enhanced electrocatalytic performance towards formic acid electrooxidation

Jingfang Zhang, You Xu and Bin Zhang*

3D Pd-P nanoparticle networks (NNs) have been successfully synthesized using a facile one-step soft-template-assisted method. The as-prepared Pd-P NNs exhibit markedly improved activity and stability towards formic acid electrooxidation over Pd NNs, commercial Pd/C and Pd-P nanoparticle aggregates (NAs).

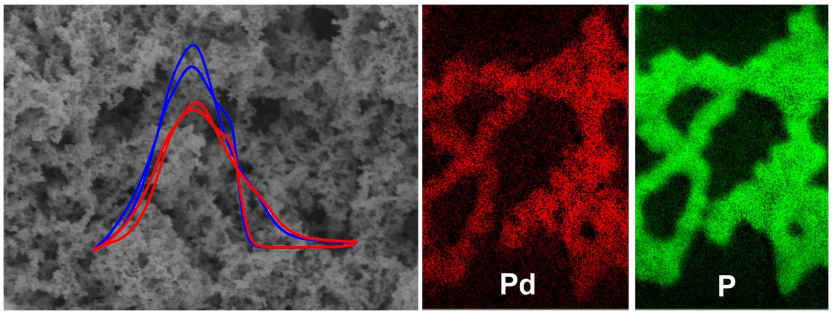

ChemComm Accepted Manuscript